ELSEVIER

Catalysis Today 32 (1996) 215–222

CATALYSIS TODAY

In situ-electron spin resonance: a useful tool for the investigation of vanadium phosphate catalysts (VPO) under working conditions

Angelika Brückner *, Bernd Kubias, Bernhard Lücke

Institut für Angewandte Chemie Berlin-Adlershof e. V., Rudower Chaussee 5, D-12484 Berlin, Germany

Abstract

Differently prepared $(VO)_2P_2O_7$ phases and an amorphous $V^{3+}PO$ catalyst were investigated under conditions of the selective *n*-butane oxidation and the toluene ammoxidation, respectively, using a self-constructed in situ-ESR flow reactor in the X-band. By examining the temperature dependence and the line shape of the ESR signals exchange integrals as well as the 2nd and the 4th moment were obtained. These parameters characterize the spin–spin exchange behaviour and, thus, structural and electronic disorder of the catalysts. Increasing structural disorder was found to improve the catalytic performance in the *n*-butane oxidation. For both catalytic processes a significant reversible alteration of the ESR line shape was observed under working conditions which is discussed in terms of a perturbation of exchange interactions between neighbouring vanadyl centres near the surface the oxidation state of which is assumed to fluctuate between +4 and +5 during the catalytic reaction.

Keywords: In situ; Electron spin resonance; Vanadium phosphate catalysts (VPO); Working conditions

1. Introduction

Vanadium phosphates (VPO) are known to catalyze both the selective oxidation of *n*-C_4 hydrocarbons to maleic anhydride (MA) [1] and the ammoxidation of methylaromatics to the corresponding imides and nitriles as well [2]. Vanadyl pyrophosphate, $(VO)_2P_2O_7$, is one of the most effective catalysts for these reactions among a wide variety of VPO compounds. Numerous papers on its catalytic and structural properties have been published in the past. However, for both catalytical processes the nature of the active sites and the various steps of the reaction mechanisms are still ambiguous. In situ investigations under working conditions should provide more insight into the changes occurring with the catalysts during reaction but such studies are rather rare in the scientific literature. Only few examples exist in which Raman spectroscopy [3] and electron microscopy [4], respectively, were employed in situ. To our knowledge, ESR measurements of (VPO) catalysts during both the selective oxidation of *n*-butane to MA and the ammoxidation of toluene to benzonitrile have never been done so fare. One reason might be that the required experimental equipment is not commercially available. Moreover, in ESR spectra of pure paramagnetic substances like vanadium(IV) phosphates *g* and hyperfine tensors are not

* Corresponding author.

PII S0920-5861(96)00077-6

resolved due to line broadening caused by dipolar and exchange interactions. Thus, a considerable part of information is lost.

In this paper we shall demonstrate a different approach to overcome this disadvantage. By examining the temperature dependence and the line shape of the ESR signals we obtained parameters characterizing the spin–spin exchange behaviour and, thus, structural disorder of differently prepared $(VO)_2P_2O_7$ phases and an amorphous ($V^{3+,4+}$PO) catalyst. These parameters are related to the catalytic activity and selectivity in the *n*-butane oxidation. Using a self-constructed flow reactor we shall show that in situ-ESR experiments in the X-band can provide useful information on changes of valence state and electronic disorder in the (VPO) catalysts during reaction.

2. Experimental

2.1. Catalysts

The precursor $VOHPO_4 \cdot 0.5H_2O$ was obtained by evaporating an aqueous solution of V_2O_5, H_3PO_4 and oxalic acid as described elsewhere [5]. The $(VO)_2P_2O_7$ catalysts were prepared from this precursor by calcination in nitrogen atmosphere for 2 h at 753 K (sample 1) and 4 h at 943 K (sample 2). Additional calcination of sample 1 for 18 days at 1073 K in argon atmosphere led to sample 3. Moreover, an industrial $(VO)_2P_2O_7$ catalyst provided by the Consortium für Elektrochemische Industrie, München, was investigated (sample 4). In this case the $VOHPO_4 \cdot 0.5H_2O$ precursor was prepared after the so called 'organic route' from a suspension of V_2O_5, H_3PO_4 and H_3PO_3 in isobutanol [6]. The catalyst investigated in this work had been equilibrated and used under butane oxidation conditions for 2000 h at 653 K.

The amorphous (V^{3+}PO) catalyst was prepared by thermal decomposition of $VO(H_2PO_3)_2$ as described elsewhere [7]. The vanadium oxidation number was initially 3.06 but increased under butane oxidation conditions (4.5 h at 753 K) to 3.41 indicating the oxidation of 41% of the vanadium to V^{4+}.

2.2. Methods

ESR measurements were performed with the cw spectrometers ERS 300 in the X-band and ERS 200 in the Q-band (Zentrum für Wissenschaftlichen Gerätebau Berlin). Variation of temperature (93 < 293) was done with the temperature control unit TEL 2 (Zentrum für Wissenschaftlichen Gerätebau Berlin). For in situ measurements (investigation of the catalyst under working conditions in the cavity of the spectrometer) a modified self-constructed ESR flow reactor was used in the X-band (Fig. 1) [8]. It consists of a reaction tube of 3 mm inner diameter equipped with a bifilar heating winding of 0.1 mm Pt wire on the outside which was placed by ground joints into an evacuated dewar for protecting the ESR cavity from high temperatures. The temperature was controlled using the temperature programmer Eurotherm 902-904 and a Ni/Cr-Ni thermocouple. The gas flow through the sample tube was adjusted with a system of mass flow controllers and thermostated saturators. For the selective *n*-butane oxidation the feed contained 1.5% *n*-butane in air. In each run 190 mg catalyst particles (0.5–1 mm) were treated with a gas flow of 300 ml h^{-1}. For toluene ammoxidation, the molar ratio of the feed components was toluene:air:NH_3:H_2O = 1:31:4.5:24.3. In each run 400 mg catalyst particles (0.5–1 mm) were treated with a gas flow of 980 ml h^{-1}.

Catalytic activities and selectivities for the *n*-butane oxidation were determined in integral reactors (7–20 g catalyst particles, 1.25–2.5 mm). The space velocities were varied between 340 and 6000 h^{-1} from 430 to 500°C. The partial oxidation products and the butane consumption were determined by gas chromatography. The carbon oxides were measured by NDIR

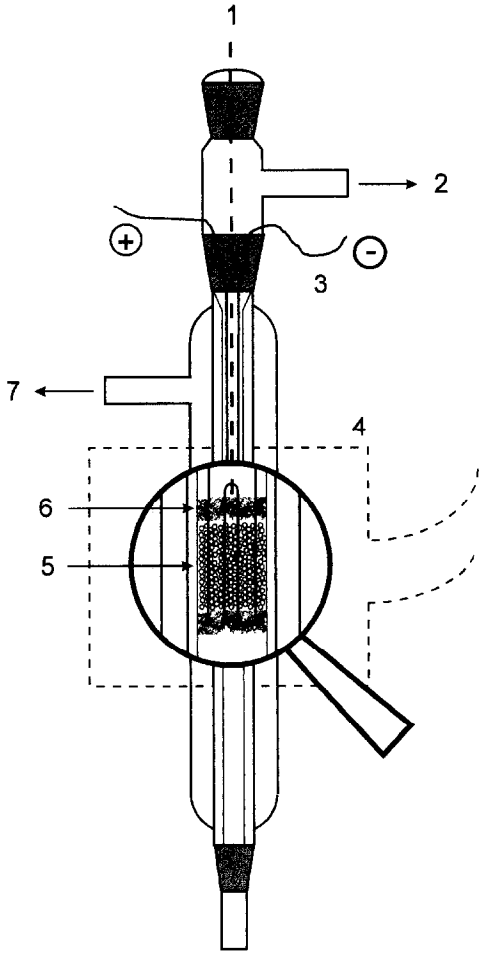

Fig. 1. ESR-in situ-flow reactor: 1, thermocouple; 2, connection to gas dosing apparatus; 3, bifilar Pt-winding; 4, cavity; 5, catalyst; 6, quartz wool; 7, connection to isolation vacuum.

photometry. The vanadium valence state was determined by potentiometric titration [9].

2.3. ESR spectra evaluation

The ESR spectra of all samples investigated consist of single lorentzian lines which are narrowed due to effective spin–spin exchange interactions between neighbouring VO^{2+} centres of the structure. For the same reason, the anisotropic g and hfs tensors are not resolved. However, from the temperature dependence of the ESR line intensity the exchange integrals, $|J|$, can be calculated using a cluster model which describes residual antiparallel ordering of nearest neighboured spins (clusters) in antiferromagnetic systems above the Neel point. The procedure for extracting these parameters from a series of ESR spectra in the range 77–293 K is described elsewhere [10,11].

In addition, the line shape was analyzed by calculating the 2nd and the 4th moment of the ESR absorption signals [12]. According to Van Vleck [13], the 2nd moment, $\langle B^2 \rangle$, is determined by dipole–dipole interactions whereas spin–spin exchange additionally contributes to the 4th moment, $\langle B^4 \rangle$. Thus, the quotient $\langle B^4 \rangle / \langle B^2 \rangle^2$ is another suitable parameter to characterize differences in the exchange behaviour of (VPO) catalysts. Both parameters, $|J|$ and $\langle B^4 \rangle / \langle B^2 \rangle^2$, are related to the degree of disorder in the various samples.

3. Results and discussion

3.1. Structural disorder and catalytic properties of $(VO)_2P_2O_7$

The various $(VO)_2P_2O_7$ samples were obtained from the $VOHPO_4 \cdot 0.5H_2O$ precursor by dehydration. It will be shown below that the calcination conditions are of great importance for the degree of structural disorder in the final $(VO)_2P_2O_7$ catalysts which itself influences their catalytic properties.

The ESR spectrum of the $VOHPO_4 \cdot 0.5H_2O$ precursor consists of an isotropic line which is narrowed due to effective spin–spin exchange interactions within the face sharing VO^{2+} dimers of the structure [14] (Fig. 2). During dehydration these dimers are cleaved and infinite ladder like double chains of VO_6 octahedra characterizing the $(VO)_2P_2O_7$ structure are formed in a topotactic reaction [14]. At the conversion point the ESR precursor signal drastically broadens and looses intensity before the pyrophosphate signal develops. The latter is exchange narrowed, too, but in this case the exchange does not proceed within dimers but along

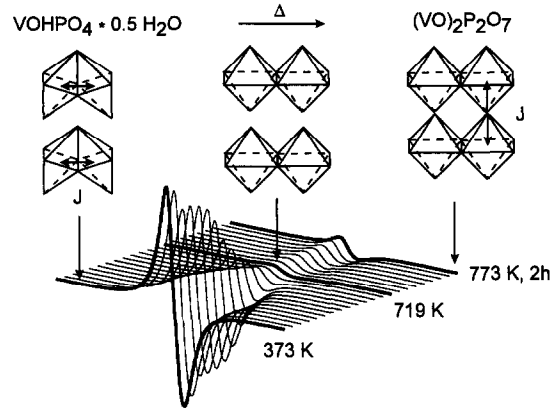

Fig. 2. Dehydration of $VOHPO_4 \cdot 0.5H_2O$ to $(VO)_2P_2O_7$ followed by ESR in situ.

the double chains [15]. The vanadium valence state and, thus, the number of spins remains constant during the calcination. Hence the ESR intensity decrease in the phase transition is only due to line broadening. During the dehydration of $VOHPO_4 \cdot 0.5H_2O$ obviously an intermediate disordered state is passed in which the face sharing vanadyl dimers of the precursor are already cleaved but the infinite double chains of the $(VO)_2P_2O_7$ structure are not yet formed as depicted schematically in Fig. 2. Thus, spin–spin exchange collapses and the line broadens.

The extent to which the intensity of the pyrophosphate signal approaches that of the precursor depends strongly on the efficiency of the spin–spin exchange proceeding along the infinite double chains via direct overlap of the d_{xy} orbitals which contain the unpaired electrons [15]. The exchange interaction is less effective when the arrangement of the vanadyl octahedra within the chains and, thus, the orbital overlap is disturbed. In contrast to the intrinsic disorder of the vanadium positions described by Thompson et al. [16] this kind of structural distortion can be influenced by the calcination conditions. The higher the calcination temperature and time the lower the structural distortion and the higher the exchange integrals, moment quotients and relative intensities of the pyrophosphate signal (Table 1). In highly disordered samples the line broadening leads to partial disappearance of the ESR intensity in the outer wings of the spectrum so that it can not be fully comprised by double integration (samples 1 and 2).

Catalytic testing of the samples in the selective oxidation of *n*-butane to maleic anhydride revealed that both catalytic activity and MA selectivity of the $(VO)_2P_2O_7$ catalysts are enhanced with rising structural disorder (Table 1). The beneficial influence of lattice defects on the catalytic activity of (VPO) catalysts in the butane oxidation has been frequently discussed in the literature [1] and agrees with our results whereas the selectivity of $(VO)_2P_2O_7$ catalysts is almost exclusively attributed to the (100) plane of the crystal structure and preparation routes are searched for which lead to the preferable formation of the latter [17]. This should rather require low structural distortion and is in contrast to our results suggesting that in addition to the VO_6 double octahedra sites on the (100) plane [1] selective oxidation can also occur in distorted areas of the structure presum-

Table 1
Spin–spin exchange behaviour and catalytic properties of $(VO)_2P_2O_7$: calcination temperature, T_{calcin}; relative ESR intensity, I (with respect to $I_{precursor} = 100\%$); exchange integrals, $|J|$; quotient of the 4th and the square of the 2nd moment of the ESR absorption signals, $\langle B^4\rangle/\langle B^2\rangle^2$; BET surface area, S_{BET}; area specific rate of MA formation, A; and MA selectivity, S_{MA}

Sample	T_{calcin} (K)	I (%)	$\lvert J\rvert$ (cm^{-1})	$\langle B^4\rangle/\langle B^2\rangle^2$	S_{BET} ($m^2\ g^{-1}$)	A (10^5 mol MA $m^{-2}\ h^{-1}$) [a]	S_{MA} (%) [b]
1	753	37	31.3	4.61	8.0	9.7	60
2	943	43	32.8	9.55	5.6	4.2	40
3	1073	87	34.0	20.85	0.5	1.8	12
4	653		27.5	6.51	18.0		

[a] Conversion of butane: 20% at 713 K.
[b] At 90% conversion of butane.

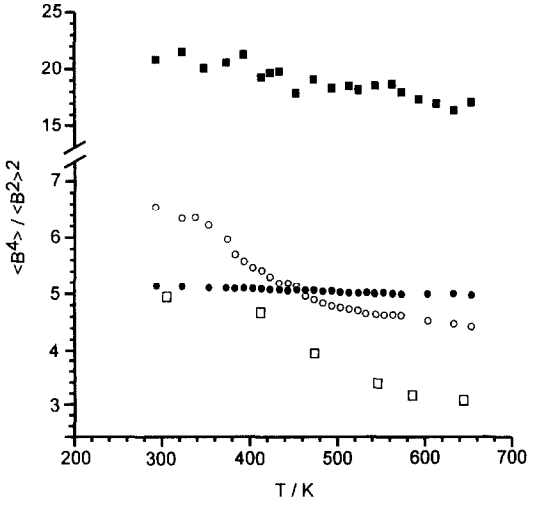

Fig. 3. Quotient of the 4th and the square of the 2nd moment of the ESR absorption signals, $\langle B^4\rangle/\langle B^2\rangle^2$, as a function of temperature in nitrogen atmosphere: ■, $(VO)_2P_2O_7$ sample 3; ○, $(VO)_2P_2O_7$ sample 4; ●, $(VO)_2P_2O_7$ sample 1; □, ($V^{3.41}$PO) catalyst after catalysis.

ably on edges, dislocations and other defect sites.

3.2. Lattice flexibility at reaction temperatures

When the various $(VO)_2P_2O_7$ samples and the amorphous ($V^{3.41}$PO) catalyst formed under butane oxidation conditions are heated in nitrogen atmosphere the moment quotient $\langle B^4\rangle/\langle B^2\rangle^2$ decreases due to thermally induced lattice vibrations which disturb spin–spin exchange. This lattice flexibility is most obvious for samples with high structural disorder like $(VO)_2P_2O_7$ prepared after the organic route and the amorphous ($V^{3.41}$PO) catalyst (Fig. 3). In the latter case the moment quotient at 673 K approaches even 3.0 which is characteristic for a gaussian line [13] indicating that exchange almost completely collapses at this temperature.

High lattice flexibility resulting from the disorder should support the oxygen transport from the bulk to the surface and vice versa. As discussed for a variety of other oxidic catalysts [18], this oxygen transport is responsible for the availability of nucleophilic oxide ions at the surface which favour the selective oxidation at higher temperatures and prevent the destruction of the carbon skeleton. Thus, it might be another reason why vanadyl pyrophosphates with a certain degree of structural disorder are more selective than well crystallized ones (Table 1).

3.3. In situ-ESR measurements during n-butane oxidation

When the various $(VO)_2P_2O_7$ samples are treated with the reaction feed of 1.5% *n*-butane in air a decrease of the moment quotient is observed (Fig. 4). This effect which is strongest for the highly disordered organically prepared sample 4 can only be observed under reaction conditions. It is reversible when the feed is replaced by nitrogen again. We explain this result in terms of a perturbation of the spin–spin exchange between the vanadyl centres near the surface during catalysis which arises because the valence state of the vanadium atoms taking part in the catalytic reaction fluctuates between +4 and +5. Numerous mechanistic discussions are based on such a redox process (e.g. [17]). However, no direct experimental evidence has been available so fare.

On the other hand, heating the $(VO)_2P_2O_7$ catalysts in pure air leads to improved exchange interactions as comprised by increasing moment

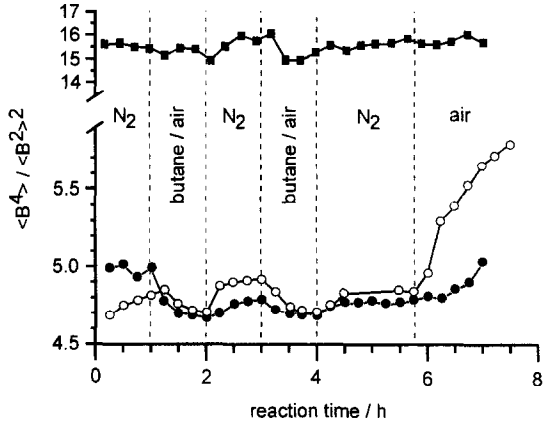

Fig. 4. Quotient of the 4th and the square of the 2nd moment of the ESR absorption signals, $\langle B^4\rangle/\langle B^2\rangle^2$, as a function of temperature during selective oxidation of *n*-butane: ■, $(VO)_2P_2O_7$ sample 3; ○, $(VO)_2P_2O_7$ sample 4; ●, $(VO)_2P_2O_7$ sample 1.

quotients (Fig. 4). This effect is not reversible when nitrogen is passed over the sample again. We suppose that lattice defects are healed in the presence of oxygen. Thus, structural disorder is diminished. The healing process is most effective in sample 4 in agreement with the above discussed oxygen transport ability. In contrast, in the highly ordered, well crystallized sample 3 no such effect was observed.

The (V^{3+}PO) catalyst reaches its maximum activity after 20 min at 753 K. For *n*-butane conversion between 10% and 70% the MA selectivity remains practically constant at 44% [7]. When this reaction is followed by in situ-ESR, the growth of a broad V^{4+} signal without hyperfine structure is observed during the catalytic reaction (Fig. 5a). The vanadium oxidation number increases from 3.06 (calcined catalyst) to 3.41 after 4.5 h time on stream. Apparently, even from the very beginning of the reaction

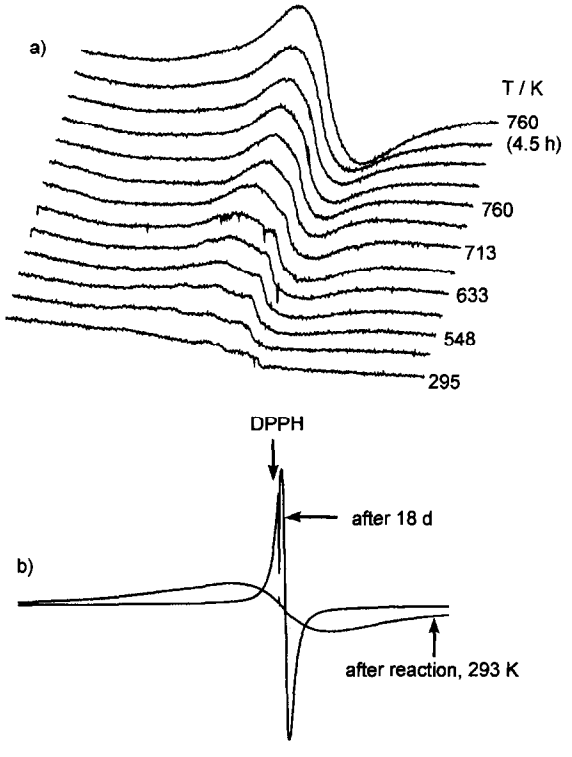

Fig. 5. (a) Development of the V^{4+} ESR signal (spectrum range 30–530 mT) in the (V^{3+} PO) catalyst during the selective oxidation of *n*-butane to MA. (b) ESR spectrum of the used catalyst ($V^{3.41}$PO) immediately after reaction and after 18 days.

closely neighbouring V^{4+} ions are formed. Mechanistic models for $(VO)_2P_2O_7$ are based on the assumption that adjacent VO^{2+} centres are required for the conversion of *n*-butane to MA in a series of consecutive steps [17]. We think that in the case of (V^{3+}PO) a similar arrangement of such centres is created in contact with oxygen from the reaction gas feed. When their concentration on the surface is sufficiently high the catalyst becomes active and selective. After cooling to 293 K an isotropic ESR signal with 109.6 mT peak-to-peak line width was recorded. However, when the catalyst is stored at room temperature a slow line narrowing becomes evident. After 18 days a peak-to-peak line width of 9.8 mT is measured which is similar to that of $(VO)_2P_2O_7$ ($\Delta B_{pp} \approx 9.0$ mT, depending on the preparation conditions) (Fig. 5b). Obviously, some kind of structural rearrangement takes place in the catalyst structure which leads to increasing exchange interactions between neighbouring V^{4+} centres. As discussed above, this rearrangement process is reversible on heating. Spin–spin exchange collapses again above 500 K indicating a fairly high degree of structural flexibility as likewise observed for highly disordered $(VO)_2P_2O_7$ (Fig. 3).

Similarities between $(VO)_2P_2O_7$ and ($V^{3.41}$PO) concerning the local symmetry of VO^{2+} centres become also evident from the Q-band ESR spectra in which the g anisotropy is resolved. The *g*-tensor components and line width of $(VO)_2P_2O_7$ sample 4 ($g_{\|} = 1.9220$, $\Delta B_{\|} = 10.0$ mT, $g_{\perp} = 1.9765$, $\Delta B_{\perp} = 7.0$ mT) and ($V^{3.41}$PO) ($g_{\|} = 1.9300$, $\Delta B_{\|} = 9.0$ mT, $g_{\perp} = 1.9800$, $\Delta B_{\perp} = 8.0$ mT) are in the same order of magnitude indicating the presence of exchange coupled VO^{2+} centres in both systems.

3.4. In situ-ESR study of $(VO)_2P_2O_7$ during the ammoxidation of toluene

First of all we have studied the interaction of sample 1 with the ammoxidation feed compo-

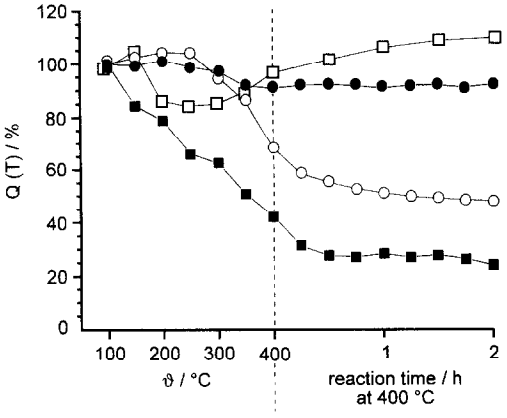

Fig. 6. Relative intensity of the $(VO)_2P_2O_7$ ESR signal, $Q(T)$, in the presence of ammoxidation feed components as a function of temperature and reaction time.

nents separately. The relative signal intensities, $Q(T)$, plotted in Fig. 6 were calculated according to $Q(T) = TI(T)/T_1I(T_1)$, where $I(T)$ are the experimental ESR intensities at the temperature T calculated by double integration and T_1 is a reference temperature (this work: 373 K). Thus, the temperature dependence of the intensities due to Curie's law is eliminated. For pure paramagnetic behaviour $Q(T)$ does not depend on temperature [10,11].

The relative intensity of the $(VO)_2P_2O_7$ signal decreases during the interaction with NH_3 and toluene, respectively (Fig. 6). On the one hand, this is due to the partial reduction of VO^{2+} ions to V^{3+} not being detected by ESR at $T > 4$ K. After 2 h treatment with 13 mol% NH_3 in N_2, 5% of the overall V^{4+} content was reduced to V^{3+}. Similarly, toluene was found to be oxidized by transition metal oxide catalysts even in the absence of gas phase oxygen [19]. The reduction of the catalyst surface by toluene starts at lower temperatures and goes to a deeper level than with ammonia. This is in agreement with TPD measurements of toluene over $(VO)_2P_2O_7$ in which total oxidation occurred above 353 K [20]. On the other hand, a second reason might be responsible for the intensity decrease. The V^{3+} ions appearing in the lattice after reduction by NH_3 and toluene disturb the spin–spin exchange between the VO^{2+} centres at least in the surface near layers. This makes exchange narrowing of the signals less efficient and leads to larger line width – an effect which had been observed similarly by Nakamoto et al. on partial reduction of vanadyl(IV) phosphate catalysts with *n*-butane [21]. Thus, a certain part of the ESR intensity disappears in the outer wings of the spectrum and cannot be fully comprised by double integration. When $(VO)_2P_2O_7$ is exposed to air the relative line intensity increases slightly although 4.2% of the vanadium is oxidized to ESR silent V^{5+} during a 2 h treatment at 673 K indicating that the above discussed defect healing process becomes evident.

In the ammoxidation experiment, this process is superimposed on the interaction of feed components with the catalyst surface being visible by a steady increase of the relative intensity as soon as air is supplied to the reaction gas feed (Fig. 7). When toluene is added to the feed the relative intensity decreases temporarily. This reversible effect is probably due to the strong adsorption of toluene on the catalyst surface hindering the interaction of the latter with oxygen from the feed.

Similar to the butane oxidation (Fig. 4) spin–spin exchange in $(VO)_2P_2O_7$ comprised

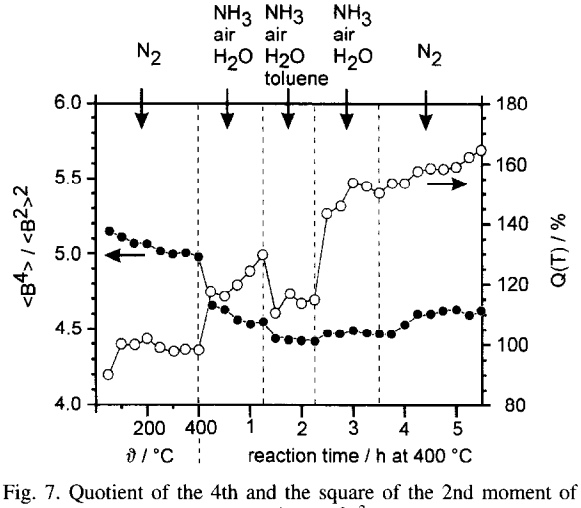

Fig. 7. Quotient of the 4th and the square of the 2nd moment of the ESR absorption signals, $\langle B^4\rangle/\langle B^2\rangle^2$, (●) and relative intensities, $Q(T)$, (○) during the ammoxidation of toluene.

by the moment quotient decreases under ammoxidation conditions, too (Fig. 7). This agrees pretty well with the proposed reaction mechanism in which a stationary redox equilibrium between vanadium centres in the valence states +3, +4 and +5 is assumed [22]. Like in the butane oxidation the fluctuation of the vanadium valence state is assumed to disturb spin–spin exchange in the surface near layers.

4. Conclusions

The exchange integrals, $|J|$, and the moment quotients, $\langle B^4\rangle/\langle B^2\rangle^2$, obtained by evaluating the temperature dependence and line shape of the ESR signals are sensitive parameters to characterize the spin–spin exchange behaviour in vanadyl(IV) phosphate catalysts which is a measure for the degree of structural and electronic disorder itself.

In $(VO)_2P_2O_7$ structural disorder depends strongly on the preparation pathway. In highly disordered samples obtained under weak calcination conditions thermal lattice vibrations gain influence at elevated temperatures as comprised by reversibly decreasing moment quotients. They are assumed to support oxygen transport and, thus, to be a reason why disordered samples have a better catalytic performance than well crystallized ones. In both catalytic processes butane oxidation and toluene ammoxidation as well a reversible perturbation of spin–spin exchange in the surface near layers has been observed which is caused by a fluctuation of the vanadium valence states being a direct evidence for the participation of surface vanadyl ions in the catalytic redox reaction.

In the (V^{3+}PO) catalyst a $(VO)_2P_2O_7$ like local arrangement of neighboring vanadyl centres develops under reaction conditions as indicated by the similar g tensors and line width derived from the ESR Q-band spectra. This is supposed to be the reason why this amorphous phase also catalyzes the oxidation of *n*-butane to maleic anhydride.

Acknowledgements

We thank the Consortium für Elektrochemische Industrie, München, for providing the industrial $(VO)_2P_2O_7$ catalyst and the Bundesministerium für Bildung, Wissenschaft, Forschung und Technologie (project no. 03D0024D4 and 03D0001B0) for financial support. Moreover, we thank Mr. G.-U. Wolf for his kind support in catalyst preparation and analysis.

References

[1] G. Centi, Editor, Catal. Today, 16 (1993) 1–153.
[2] A. Martin, B. Lücke, H. Seeboth and G. Ladwig, Appl. Catal., 49 (1989) 205.
[3] F. Ben Abdelouahab, R. Olier, N. Guilhaume, F. Lefebvre and J.C. Volta, J. Catal., 134 (1992) 151.
[4] P.L. Gai and K. Kourtakis, Science, 267 (1995) 661.
[5] K. Schlesinger, M. Meisel, G. Ladwig, B. Kubias, R. Weinberger and H. Seeboth, Zentralinstitut für Anorganische Chemie, Berlin, DD WP 256659 Al, (23/10/1984).
[6] K. Neubold and K.-D. Gollmer, Chemische Werke Hüls, AG DE 3010710 (20/03/1980).
[7] G.-U. Wolf, B. Kubias, H. Worzala and M. Meisel, Chem. Ing. Technol., 66 (1994) 951.
[8] H.G. Karge, J.P. Lange, A. Gutze and M. Laniecki, J. Catal., 114 (1988) 144.
[9] M. Niwa and Y. Murakami, J. Catal., 76 (1982) 9.
[10] A. Brückner, G.-U. Wolf, M. Meisel and R. Stößer, Eur. J. Solid State Inorg. Chem., 30 (1993) 801.
[11] K. Dräger, Z. Naturforsch. A, 32 (1977) 163.
[12] C.P. Poole, Jr., Electron Spin Resonance: A Comprehensive Treatise on Experimental Techniques, Interscience Publishers, New York, 1967.
[13] J.H. Van Vleck, Phys. Rev., 74 (1948) 1168.
[14] J.W. Johnson, D.C. Johnston, A.J. Jacobson and J.F. Brody, J. Am. Chem. Soc., 106 (1984) 8123.
[15] G. Villeneuve, P. Amros, D. Beltran and D. Drillon, NATO ASI Ser., Ser. B (Org. Inorg. Low-Dimens. Cryst. Mater.), 168 (1987) 417.
[16] M.R. Thompson, A.C. Hess, J.B. Nicholas, J.C. White, J. Anchell and J.R. Ebner, Stud. Surf. Sci. Catal., 82 (1994) 167.
[17] E. Bordes, Catal. Today, 16 (1993) 27.
[18] A. Bielanski and J. Haber, Oxygen in Catalysis, Marcel Dekker, New York, 1991.
[19] A.B. Azimov, V.P. Vislowskii, E.A. Mamedov and R.G. Rizaev, J. Catal., 127 (1991) 354.
[20] K. Büker, Institut für Angewandte Chemie Berlin- Adlershof e. V., private communication.
[21] M. Nakamoto, K. Kawai and Y. Fujiwara, J. Catal., 34 (1974) 345.
[22] A. Martin, H. Berndt, B. Lücke and M. Meisel, Topics Catal., submitted.